JES

JOURNAL OF ENVIRONMENTAL SCIENCES

ISSN 1001-0742
CN 11-2629/X

July 1, 2013 Volume 25 Number 7
www.jesc.ac.cn

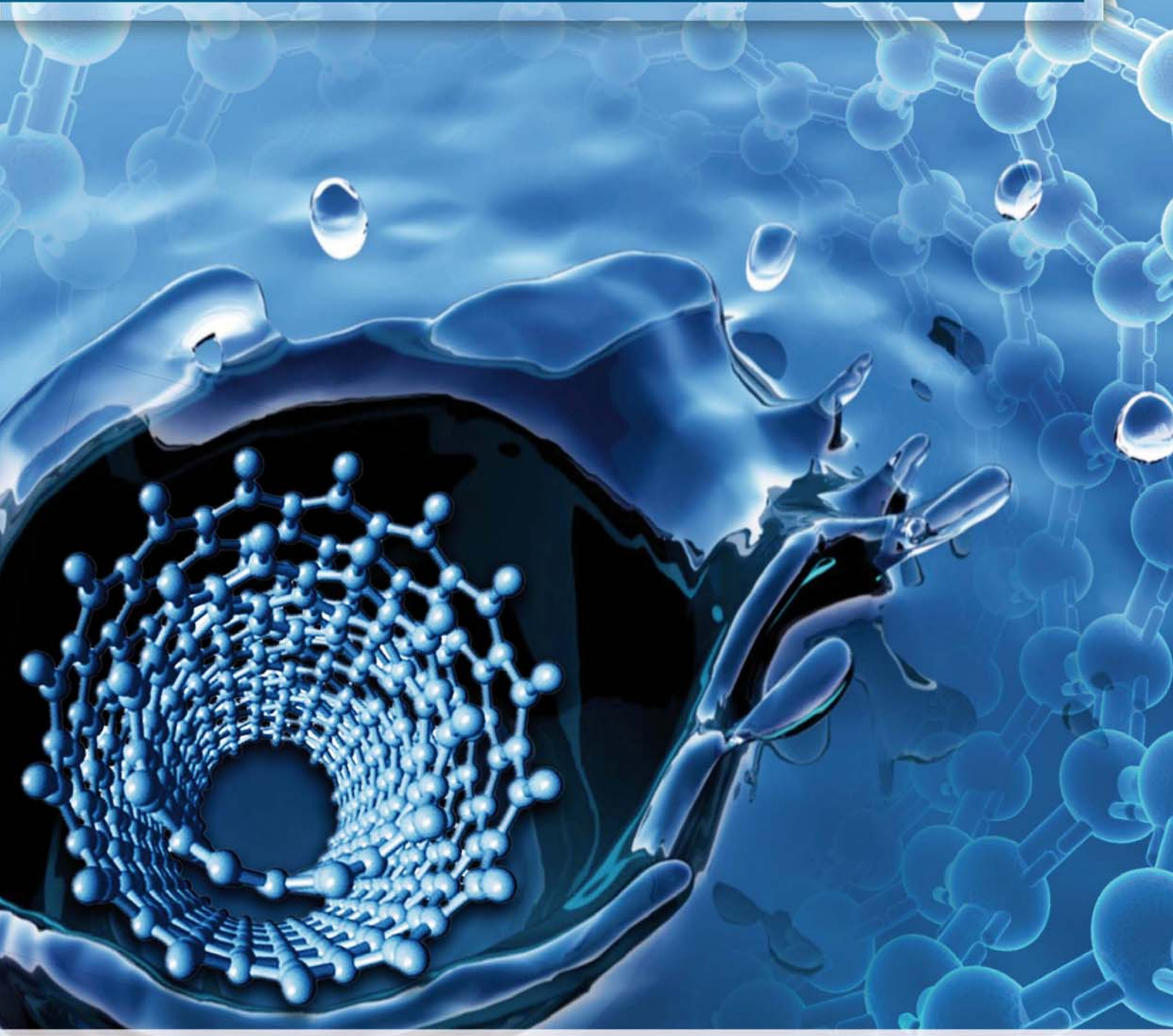

ELSEVIER

Science Press

Sponsored by
Research Center for Eco-Environmental Sciences
Chinese Academy of Sciences

ISSN 1001–0742 **Journal of Environmental Sciences** Vol. 25 No. 7 2013

CONTENTS

Environmental health and toxicology

Environmental catalysis and materials

The 8th International Conference on Sustainable Water Environment

Serial parameter: CN 11-2629/X*1989*m*237*en*P*28*2013-7

Available online at www.sciencedirect.com
ScienceDirect
Journal of Environmental Sciences 2013, 25(7) 1291–1299
JOURNAL OF ENVIRONMENTAL SCIENCES
ISSN 1001-0742
CN 11-2629/X
www.jesc.ac.cn

Factors influencing antibiotics adsorption onto engineered adsorbents

Mingfang Xia[1,2], Aimin Li[1,*], Zhaolian Zhu[1], Qin Zhou[1], Weiben Yang[3]

1. State Key Laboratory of Pollution Control and Resources Reuse, School of the Environment, Nanjing University, Nanjing 210093, China. E-mail: mingfang_xia@sina.com
2. General Office of Lake Taihu Water Pollution Prevention and Control of Jiangsu Province, Nanjing 210024, China
3. School of Chemistry and Materials Science, Nanjing Normal University, Nanjing 210097, China

Received 18 October 2012; revised 23 January 2013; accepted 24 January 2013

Abstract

The study evaluated the adsorption of two antibiotics by four engineered adsorbents (hypercrosslinked resin MN-202, macroporous resin XAD-4, activated carbon F-400, and multi-walled carbon nanotubes (MWCNT)) from aqueous solutions. The dynamic results demonstrated the dominant influence of pore size in adsorption. The adsorption amounts of antibiotics on XAD-4 were attributed to the hydrophobic effect, whereas steric hindrance or micropore-filling played a main role in the adsorption of antibiotics by F-400 because of its high microporosity. Aside from F-400, similar patterns of pH-dependent adsorption were observed, implying the importance of antibiotic molecular forms to the adsorption process for adsorbents. Increasing the ionic concentration with $CaCl_2$ produced particular adsorption characteristics on MWCNT at pH 2.0 and F-400 at pH 8.0, which were attributed to the highly available contact surfaces and molecular sieving, respectively. Its hybrid characteristics incorporating a considerable portion of mesopores and micropores made hypercross linked MN-202 a superior antibiotic adsorbent with high adsorption capacity. Furthermore, the adsorption capacity of MWCNT on the basis of surface area was more advantageous than that of the other adsorbents because MWCNT has a much more compact molecular arrangement.

Key words: adsorption; resin; carbon nanotubes; pore size; surface area

DOI: 10.1016/S1001-0742(12)60215-0

Introduction

Antibiotics are used extensively in human and veterinary medicine for disease control and in livestock feed. Inevitably, they are discharged into aquatic environments via domestic wastewater effluent with concentrations in the μg-per-liter range, from disposal of expired pharmaceuticals, and excretion as original or metabolized forms (Ternes et al., 2004). Some researchers have demonstrated the removal of antibiotics using natural adsorbents such as humic substances (Richter et al., 2009), organic materials (Kahle and Stamm, 2007a), clay minerals (Thiele-Bruhn et al., 2004; Gao et al., 2005; Kahle and Stamm, 2007b), and soils (Kurwadkar et al., 2007; Sanders et al., 2008; Braschi et al., 2010). In these previous studies, adsorption was primarily driven by specific mechanisms involving cation exchange (Richter et al., 2009) and surface complexation reactions (Thiele-Bruhn et al., 2004; Gao et al., 2005; Kahle and Stamm, 2007a) (H-bonding and other polar interactions) between multifunctional antibiotic molecules and corresponding interactive sites of the adsorbents. Antibiotics speciation and the surface charge density of adsorbents are the most important determinants of adsorption (Thiele-Bruhn et al., 2004; Kurwadkar et al., 2007; Sanders et al., 2008; Braschi et al., 2010). However, the relative importance of surface area and pore size in the adsorption of antibiotics on these adsorbents has not been evaluated.

Due to their large surface areas and controllable pore size distributions, engineered adsorbents such as carbon nanotubes, activated carbons, and porous resins have shown great potential in removing undesirable organic contaminants from aqueous solutions. Among them, carbon nanotubes are considered to be a good choice because their structures are well defined and their surfaces are relatively uniform in contrast to activated carbon and porous resins (Yang et al., 2010). Engineered carbon nanotubes are extensively employed to remove emerging organic contaminants from aqueous media and tend to adsorb antibiotics very strongly (Ji et al., 2009a, 2010a; Oleszczuk et al., 2009; Zhang et al., 2010). A mechanism involving electrondonoracceptor interactions and cation-π bonding between the compounds and the surface of carbon

* Corresponding author. E-mail: liaimin99@vip.163.com

nanotubes has been proposed in previous studies. Although activated carbon and porous resins have been persistently utilized in treating and recovering wastewater (Valderrama et al., 2011), studies addressing antibiotics adsorption by activated carbon and resins are still scarce (Choi et al., 2008; Ji et al., 2009b, 2010b; Domínguez et al., 2011), thereby limiting the knowledge needed to assess their adsorption capacities and explore their applications. Moreover, the mechanism and adsorption behavior of antibiotics onto engineered adsorbents under the same conditions are largely unknown. Removing antibiotics from water using engineered adsorbents requires a deep understanding of adsorption interactions and the relative importance of their surface areas and pore sizes in the adsorption process.

The objective of the present study is to investigate the adsorption behavior and predominant factors controlling the adsorption of antibiotics to well-known engineered adsorbents. Hypercrosslinked resin MN-202, macroporous resin XAD-4, coal-based granular activated carbon Filtrasorb-400 (F-400), and multiwalled carbon nanotubes (MWCNT) were selected as adsorbents. Two commonly used antibiotics, sulfapyridine (SPY) and sulfadimethoxine (SDM), were examined as adsorbates in batch adsorption experiments. SPY and SDM have similar water solubility and p$K_{a,1}$ (2.3 vs. 2.4), but different partition coefficients K_{ow} (logK_{ow} values were 0.35 vs. 1.63) and p$K_{a,2}$ (8.4 vs. 6.0) (Gao et al., 2005; Sanders et al., 2008). They are amphoteric molecules and may also undergo pH-dependent speciation reactions, which suggests that the distribution coefficient of ionizable species is a more relevant parameter. Therefore, pH is expected to be a key chemical factor affecting the adsorption of sulfonamides to engineered adsorbents. The effects of solution chemistry conditions (pH, ionic strength, and temperature) on adsorption were evaluated. The present study is the first focusing on the adsorption of sulfonamide antibiotics to different well-known engineered adsorbents.

1 Materials and methods

1.1 Adsorbates and adsorbents

SDM and SPY (99%) were obtained from Sigma-Aldrich Chemical Co. (Shanghai, China) and used as received. Water used in the study was purified by distillation.

Commercially available resin MN-202 was supplied by the Shanghai Office, Purolite International Co., Ltd. Commercial resin XAD-4 (Rohm-Haas Co., USA) and granular F-400 (Calgon Carbon Co., USA) were purchased from the Shanghai reagent vendors. The carbon nanotubes (outer diameter 8–15 nm, length 20 μm, inner pore diameter, 3–4 nm purity > 95 wt.%) were obtained from Chengdu Organic Chemicals Co., Ltd., Chinese Academy of Sciences. Nitrogen adsorption and desorption experiments were carried out at 77 K to determine the surface properties of the adsorbents. The Brunauer-Emmett-Teller (BET) surface area was calculated from adsorption-desorption isotherms using the standard BET equation. All calculations were performed automatically by an accelerated surface area and porosimeter system (ASAP 2010, Micromeritics, USA).

1.2 Adsorption assay

An adsorbent (0.05 g) was introduced to a series of 150 mL conical flasks, and 100 mL of sulfonamides in an aqueous solution was added to each flask. The flasks were then completely sealed and placed in an incubator shaker (New Brunswick, Model G25) at a pre-set temperature and a shaking speed of 130 r/min. The pH of the solution was adjusted using 0.01 mol/L HCl or NaOH. In the ionic strength experiments, adsorption was performed using background solutions of 0%, 1%, 3%, 5%, 7%, and 9% NaCl and $CaCl_2$ (mass concentration). To obtain kinetic data and determine the time required for equilibrium to occur after adsorption, 100 mL of sulfonamide solution was introduced to a series of 150 mL conical flasks. The initial concentration of sulfonamide was 100 mg/L; this was shaken with 0.05 g of adsorbent and sampled at different time intervals at 303 K. The concentrations of SDM and SPY in the solutions were quantified after equilibrium using HPLC with an ultraviolet detector at 361 and 367 nm, respectively. The mobile phase was composed of a phosphoric acid/acetonitrile mixture (83:17, *V/V*) and the flow rate was 1 mL/min. The detection limits were set at 0.05 mg/L. Adsorption data were collected in triplicate for the pH and salt concentration experiments and in duplicate for all other experiments. The adsorption capacity, q_e (mg/g), was calculated using Eq. (1):

$$q_e = V(C_0 - C_e)/m \quad (1)$$

where, C_0 (mg/L) is the initial sulfonamide concentration, C_e (mg/L) is the residual sulfonamide concentration at equilibrium, V (L) is the volume of solution, and m (g) is the mass of dry adsorbents.

2 Results and discussion

2.1 Characteristics of the adsorbents

Four adsorbents with different physicochemical properties were characterized. The BET surface area of MN-202 (1155.8 m^2/g) was the largest, while those of XAD-4, F-400, and MWCNT were 880, 877.8, and 174.0 m^2/g, respectively. The two resins showed a similar average pore diameter (5.19 and 5.8 nm), larger than the other two adsorbents. The pore structure of F-400 and XAD-4 presented a distinct difference; the former had the largest micropore area (761.8 m^2/g) and the lowest average pore diameter (2.27 nm), whereas the latter presented the largest average pore diameter and the least micropore area (39.0 m^2/g), indicating that F-400 and XAD-4 dominate the

micropore and mesopore regions, respectively. Following the literature (Yang et al., 2007, 2010), the MWCNT used in the present experiment had an elemental carbon content of +99.8%; its surface was hydrophobic without any functional groups, consistent with that of the macroporous resin XAD-4.

2.2 Adsorption kinetics

Figure 1 compares the adsorption kinetics of sulfonamides between the four adsorbents at pH of 2.0. Both SDM and SPY demonstrated relatively fast sorption kinetics on XAD-4 and MWCNT. Apparent equilibrium was reached in about 48 hr, but 80%–95% of the total adsorbed compounds were achieved during the initial 20 hr. The adsorption of SDM and SPY by MN-202 and F-400 was characterized by two processes of different kinetics: as a fast initial adsorption to the surface mesopores and macropores, followed by a slow diffusion into micropores.

To evaluate the kinetic adsorption mechanism, the pseudo first-order, pseudo second-order, and intra-particle diffusion models were tested. Only the pseudo second-order model provided the best match for all experimental data.

$$\frac{t}{q_t} = \frac{1}{k_1 q_e^2} + \frac{t}{q_e} \quad (2)$$

where, q_e (mmol/g) and q_t (mmol/g) are the amounts of sulfonamides adsorbed at equilibrium and time t (hr), respectively; and k_1 (g/(mmol·hr)) is the pseudo second-order rate constant. The plots show that the regression coefficients are higher than 0.988 for all adsorbates and adsorbents (**Table 1**).

The values of the constant k_1 for SDM and SPY adsorption onto XAD-4 and MWCNT were clearly greater than those onto MN-202 and F-400, which may directly relate to the adsorption rate and the parameters t_{80}. Adsorbate molecules may be able to fit into the macropore surface faster than wedge into the micropore area; sulfonamides cannot enter small micropores smoothly. Therefore, the adsorption diffusion of the molecules within the micropores of MN-202 and F-400 is expected to be very slow, and because of their high microporosity, the equilibrium time for MN-202 and F-400 was greater than those for XAD-4 and MWCNT. In contrast, XAD-4 and MWCNT had ordered, open pore structures, thus allowing rapid solute diffusion into them. The fact that all the values of k_1 of SPY were greater than those of SDM certified the importance of pore size in the rate-limiting step, because the molecular surface area of SPY (65.6 Å^2) is less than that of SDM (80.1 Å^2).

Oleszczuk et al. (2009) suggested that the kinetics of organic compounds following the pseudo second-order

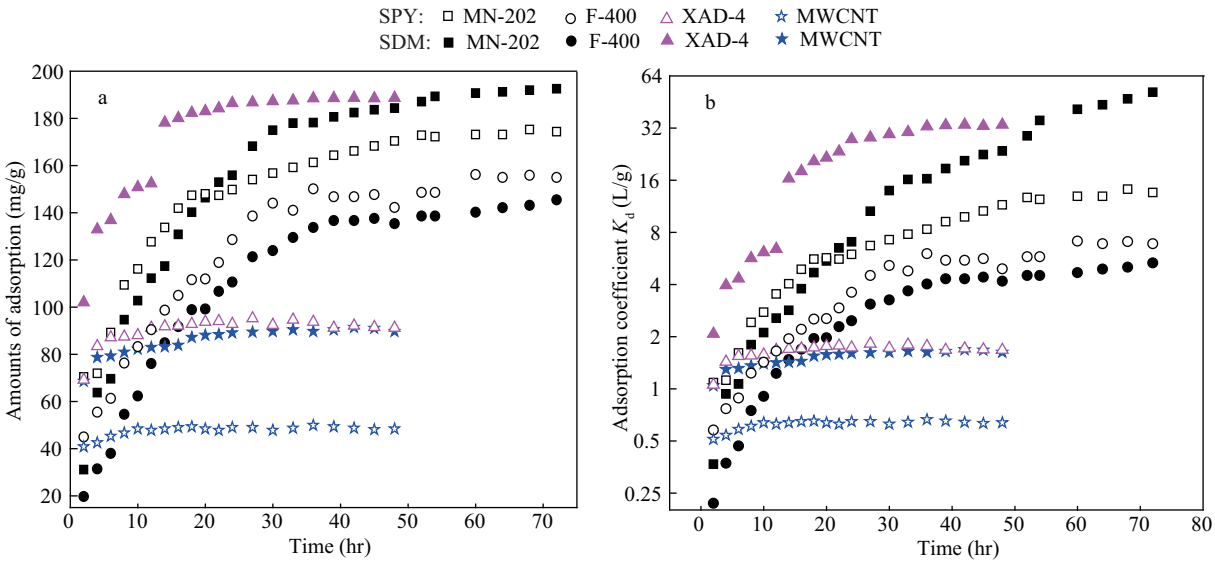

Fig. 1 Adsorption kinetics of sulfapyridine (SPY) and sulfadimethoxine (SDM) on the basis of amount of adsorption (a) and adsorption coefficients (b) on the four adsorbents at 303 K and pH 2.0; the initial concentration are all 100 mg/L.

Table 1 Calculated pseudo second-order adsorption rate constants for SDM and SPY

Adsorbents	SDM				SPY			
	q_e (mmol/g)	k_1 (g/(mmd·hr))	r^2	t_{80} (hr)	q_e (mmol/g)	k_1 (g/mmol·hr))	r^2	t_{80} (hr)
MN-202	0.732	0.121	0.997	45.3	0.757	0.229	0.999	23.1
XAD-4	0.632	0.887	0.999	7.1	0.371	12.1	0.999	0.889
F-400	0.597	0.098	0.988	68.3	0.716	0.141	0.994	39.7
MWCNT	0.296	3.724	0.999	3.6	0.197	17.6	0.999	1.16

q_e is the amounts of sulfonamides adsorbed; k_1 is the pseudo second-order rate constant; t_{80} is the time needed to reach 80% of the adsorption capacity.

model is controlled by a chemisorption process. In addition to the limiting effect of diffusion mechanisms, the main impetus in adsorption may come from adsorption interactions between the sulfonamides and the surface of the adsorbents. Considering the obvious disparity in the molecular weight of SPY and SDM, adsorption coefficients ($K_d = q_e/C_e$, L/g) were used to evaluate adsorption strength instead of adsorption amounts. After equilibrium, the adsorption coefficients K_d of SPY onto MN-202, XAD-4, and MWCNT were all less than those of SDM (**Fig. 1b**), which could be attributed to the contributions of the hydrophobic effect and hydrogen bonding. The strength of hydrophobic interaction depends on the partition coefficient (K_{ow}) of adsorbates, while that of hydrogen-bonding interaction depends on the solute hydrogen-bonding acceptor and/or donor ability. Sulfonamide contains several moieties capable of engaging in hydrogen bonding as acceptors (e.g., $-SO_2^-$, $-OCH_3$, pyrimidine N) or donors (e.g., anilinic N, sulfonamidic N). The additive effect of multiple hydrogen bonds between adsorbates and adsorbents could improve adsorption affinity (Gao and Pedersen, 2010). The partition coefficient (K_{ow}) and hydrogen-bonding acceptors of SDM molecules are greater than those of SPY, consistent with their adsorption coefficients K_d. In terms of SDM and SPY on XAD-4, their ratio of K_{ow} (19.1) is almost the same as that of K_d (18.4), indicating the predominant contribution of the hydrophobic effect. In addition, resin XAD-4 is composed of styrene divinylbenzene copolymers, which are hydrophobic in character and possess no ion-exchange capacity (Kujawski et al., 2004). Although several interactions were observed in the adsorption of sulfonamides to XAD-4 resin, the important contribution of the hydrophobic effect to the adsorption is incontrovertible. In contrast, the value of K_d for SPY on F-400 is greater than that of SDM, which negatively relates to their molecular surface area. Thus, the contribution of steric hindrance or micropore-filling is indisputable in sulfonamide adsorption by micropore-activated carbon F-400 (Costa et al., 1988; Wibowo et al., 2007).

In addition to the hydrophobic effect and hydrogen bonding, the existence of π-π electron donoracceptor interactions and/or cation-π bonding (cationic sulfonamide) between the sulfonamide molecules and the surface of the adsorbents is reasonable (Ji et al., 2009a, 2010a; Oleszczuk et al., 2009). The two tested sulfonamide antibiotics each possess one benzene ring and one aromatic heterocyclic group. The sulfonamide group between them has a strong electron withdrawing ability, causing the two aromatic rings to be electron-depleted and hence serve as effective π-electron acceptors. Electrostatic interaction between the pyrimidine ring and/or anilinium moieties of sulfonamide molecules and functional groups on the surface of MN-202 and F-400 are also conceivable (Tolls, 2001; Rabie et al., 2007). In comparison to traditional hydrophobic organic chemicals, sulfonamide adsorption (SA) is relatively more complicated because it may exist as three types of species at different pH levels, namely SA^+, SA^0, and SA^-. The cationic species (SA^+) dominates at lower pH values, the neutral form (SA^0) is the principal species at pH values between $pK_{a,1}$ and $pK_{a,2}$, and the anionic species (SA^-) is the main form at higher pH values.

2.3 Effects of pH

The adsorption of sulfonamides is related to the ionization of amphoteric sulfonamides (Sukul et al., 2008). When the pH increased from 1 to 12, SDM and SPY presented different tendencies in terms of the amounts adsorbed onto the four adsorbents (**Fig. 2**), indicating the importance of species in adsorption. The percentage of each ionic form of sulfonamides can be expressed as a function of pH and pK_a (Schwarzenbach et al., 1993). Different species of SPY and SDM from pH of 1.0 to 12.0 were calculated (**Table 2**).

At pH ⩽ 4.0, the percentages of cationic forms (SDM^+ and SPY^+) and neutral forms (SDM^0 and SPY^0) are the main species in the aqueous solutions. In this stage, the amounts of SDM and SPY adsorbed onto the four adsorbents remained almost constant (**Fig. 2**). At pH ⩾ 5.0, the percentage of the anionic form of SDM^- notably emerges (9.07%) while the percentage of SPY^- at pH 7 approaches 4%. The observed effects of pH on adsorption correlate well with the pH-regulated distribution of the protonated species of sulfonamides. As shown in **Fig. 2**, the adsorption amounts of SDM and SPY decreased with the increase in their percentages of anionic form.

To quantitatively identify the contribution of different species to the overall sulfonamide adsorption, the following empirical models can be used to calculate adsorption coefficients for individual SPY and SDM species using SPSS 17.0 (Zhang et al., 2010):

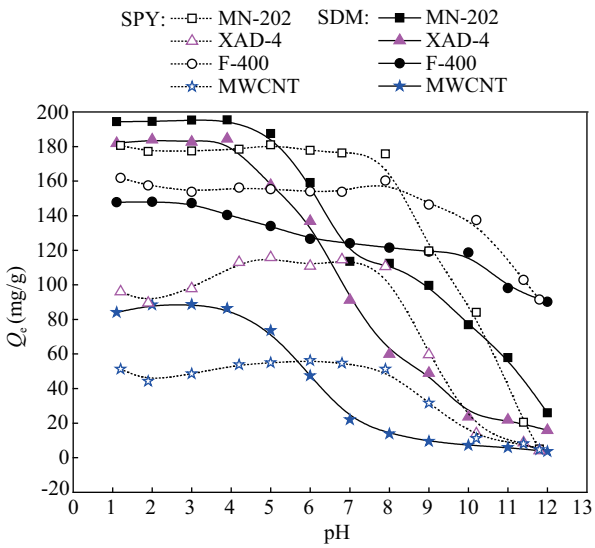

Fig. 2 Relation between pH values and adsorbed amounts of SDM and SPY onto the four adsorbents at 303 K. Initial concentrations = 100 mg/L.

Table 2 Species percentage of the two sulfonamides at different pH values

pH	1.1	2.0	3.0	3.9	5.0	6.0	7.0	8.0	9.0	10.0	11.0	12.0
SDM^+ (%)	95.2	71.5	20.0	3.0	0.23	0.01	0	0	0	0	0	0
SDM^0 (%)	4.8	28.5	79.9	96.2	90.7	49.99	9.1	0.99	0.1	0.01	0	0
SDM^- (%)	0	0	0.1	0.8	9.07	50	90.9	99.01	99.9	99.99	100	100
SPY^+ (%)	94.1	66.6	16.6	2.5	0.2	0.02	0	0	0	0	0	0
SPY^0 (%)	5.9	33.4	83.4	97.5	99.76	99.58	96.2	71.5	20.1	2.5	0.3	0.03
SPY^- (%)	0	0	0	0	0.04	0.40	3.8	28.5	79.9	97.5	99.7	99.97

$$K_d = K_d^+\delta^+ + K_d^0\delta^0 \quad 1 \le pH \le 4 \tag{3}$$

$$K_d = K_d^0\delta^0 + K_d^-\delta^- \quad 5 \le pH \le 12 \tag{4}$$

where, K_d (L/g) is the overall adsorption coefficient, and K_d^+, K_d^0, and K_d^- are the adsorption coefficients for cationic, neutral (including zwitterionic), and anionic sulfonamides, respectively. The terms δ^+, δ^0, and δ-denote the percentages of cationic, neutral, and anionic sulfonamides at a certain pH, respectively. The contributions of negatively charged sulfonamide species at pH $\leqslant$ 4.0 and positively charged sulfonamide species at pH $\geqslant$ 5.0 were neglected because of their much lower percentage.

As shown in **Table 3**, the adsorption coefficients of anionic sulfonamides (K_d^-) on MN-202, XAD-4, and MWCNT are much lower than those of neutral (K_d^0) and cationic (K_d^+) species, and the values of K_d^0 are nearly the same as those of K_d^+. This may be attributed to the deprotonation on the sulfonamide group, which could significantly decrease the π-withdrawing ability and hydrogen bonding of the group, suppressing their interactions with the surface of adsorbents (Zhang et al., 2010). Considering the higher percentages of neutral and cationic species, their contribution to the overall adsorption is much harder to ignore. Compared with the other adsorbents, MN-202 exhibits a prominent adsorption capacity toward the two adsorbates SDM and SPY. All the values of K_d^0 and K_d^+ for MN-202 are much greater than those of the other adsorbents, which could be ascribed to its high specific surface area and bimodal pore size distribution. The hypercross linked resin MN-202 presents not only high microporosity, which is similar to that of F-400, but also analogous macroporosity, similar to that of XAD-4. The suitable pore size distribution makes MN-202 a superior sulfonamide adsorbent with high adsorption capacity.

For activated carbon F-400, the effects of pH on the adsorbed amounts of sulfonamides are different from the other adsorbents. Its adsorption coefficients for anionic sulfonamides (K_d^-) remain at higher values compared with the others, illustrating that the adsorption mechanism of sulfonamides on F-400 might be dependent on pore size.

2.4 Effects of ion concentration

Figure 3 displays the effects of ionic strength (NaCl, $CaCl_2$) on SDM adsorption on the four engineered adsorbents. At pH 8.0, the trends are evident, and SDM adsorption with NaCl and $CaCl_2$ increases with the ionic concentration, except for that of F-400 with $CaCl_2$. SPY-adsorbed amounts increase with the increase in ionic concentration at pH 8.0, which could largely result from the well-known salting out effect (Zhou et al., 2006), where the solubility of SDM in water is decreased when NaCl and $CaCl_2$ are added to it. In the salting out effect, the decrease in solubility of SDM in water facilitates the diffusion of more SDM to the surface of the adsorbents and an increase in adsorption amount. Previous studies have also reported that increasing ionic strength facilitates the adsorption of ionic compounds to carbonaceous adsorbents because of the electrostatic screening of the surface charge brought about by the counterion species added (Vinu et al., 2006; Fontecha-Cámara et al., 2007). Moreover, Ca^{2+} may simultaneously bind with negatively charged SDM and interact either with negative charges or π electrons of the adsorbents via cation-π bonding (Oleszczuk et al., 2009). However, for SDM adsorption to F-400 with $CaCl_2$, the molecular sieving effect may occur either because the available pore width is narrower than the molecular size of the Ca^+-SDM^- complex or because the shape of the pores does not allow these molecules to penetrate into the

Table 3 Calculated adsorption coefficients for three species of SPY and SDM

	1.0 ⩽ pH ⩽ 4.0						5.0 ⩽ pH ⩽ 12.0					
	SDM			SPY			SDM			SPY		
	K_d^+ (L/g)	K_d^0 (L/g)	R_{adj}^2	K_d^+ (L/g)	K_d^0 (L/g)	R_{adj}^2	K_d^0 (L/g)	K_d^- (L/g)	R_{adj}^2	K_d^0 (L/g)	K_d^- (L/g)	R_{adj}^2
MN-202	67.0 ± 1.6	85.6 ± 1.5	0.999	17.6 ± 1.3	15.8 ± 1.1	0.992	28.8 ± 3.3	0.6 ± 1.4	0.907	17.3 ± 0.8	0.4 ± 0.8	0.984
XAD-4	20.7 ± 1.5	23.0 ± 1.4	0.994	1.6 ± 0.3	2.3 ± 0.3	0.969	8.2 ± 0.3	0.5 ± 0.1	0.991	2.8 ± 0.1	0.2 ± 0.1	0.985
F-400	5.8 ± 0.3	5.1 ± 0.3	0.995	8.3 ± 0.4	6.7 ± 0.4	0.996	4.3 ± 0.6	2.6 ± 0.2	0.962	7.4 ± 0.7	3.2 ± 0.7	0.943
MWCNT	1.5 ± 0.1	1.6 ± 0.1	0.998	0.6 ± 0.1	0.7 ± 0.1	0.984	1.3 ± 0.01	0.1 ± 0.01	0.992	0.8 ± 0.01	0.1 ± 0.01	0.983

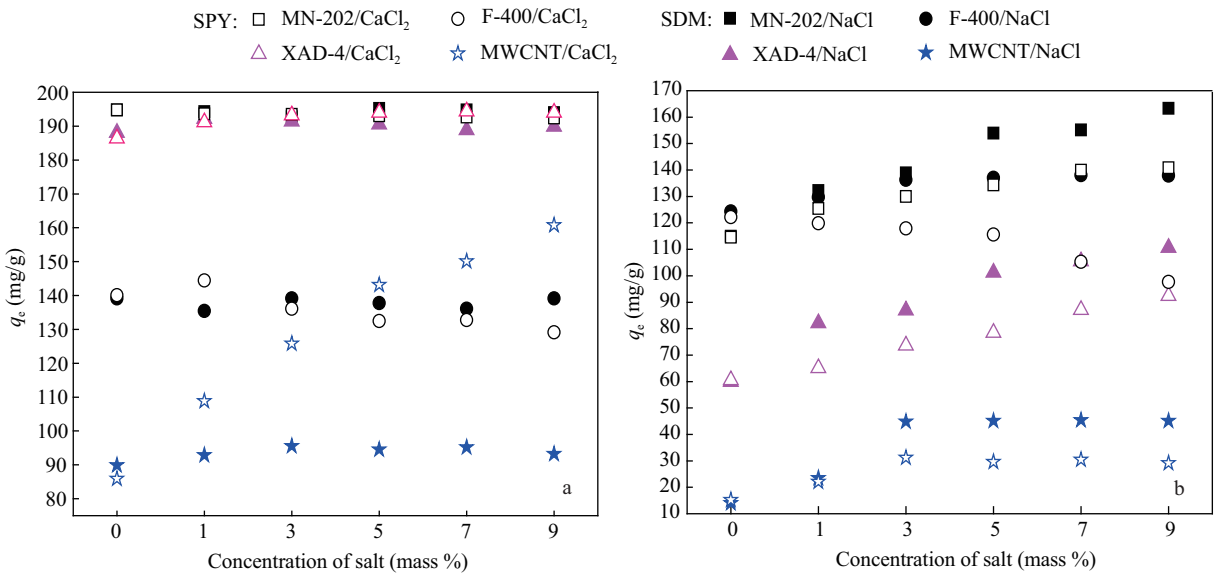

Fig. 3 Influence of ionic concentration (NaCl and $CaCl_2$) on adsorbed amounts of sulfadimethoxine at 303 K and pH = 2.0 (a) and pH = 8.0 (b). Initial concentration = 100 mg/L.

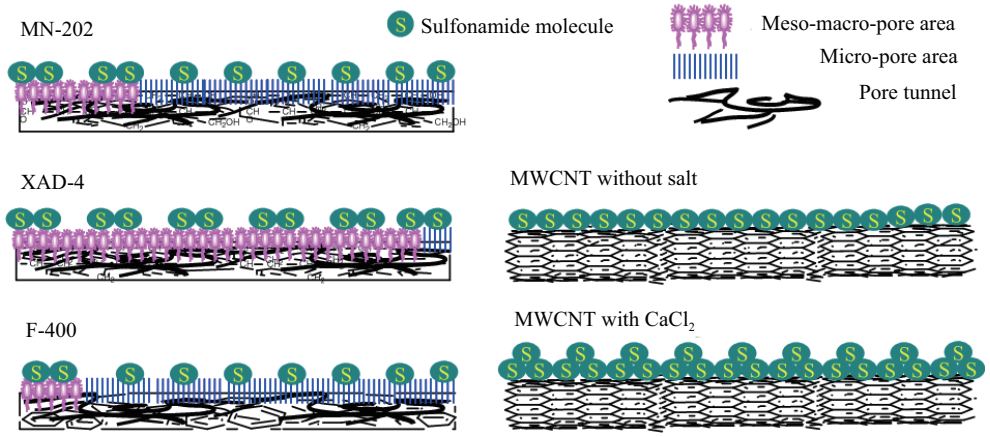

Fig. 4 Schematic diagram of possible molecule arrangement on the surface of the four adsorbents with different potential adsorption sites.

micropores of F-400 (Bandosz, 2006).

At pH 2.0, SDM adsorption with NaCl and $CaCl_2$ remained almost constant with the increase in ionic concentration, except for that of MWCNT with $CaCl_2$. An increase in ionic strength would interfere with the cation-π bonding between the cationic sulfonamide (predominant under pH 2.0) and the surface of adsorbents due to the electronic screening of cationic species by the added cation (Na^+ and Ca^{2+}), even though the salting out effect still contributes positively to the adsorption process. Currently, the adsorption sites of MN-202, XAD-4, and F-400 are known to exist mainly at the pore surface, including two-dimensional slit pores and three-dimensional cross-linked spaces. In comparison, the adsorption sites of MWCNT may be on the external surface, peripheral grooves at the boundary of bundles, interstitial pore spaces between the tubes, and inner cavities. The significant differences among their structural characteristics can be further explained by the molecular arrangement on their surfaces. An attempt to evaluate the occupied area per adsorbed SDM molecule (A_m) according to Eq. (5) was made:

$$A_m = \frac{S_{BET} \times 310.3}{A_{abs} \times N_A} \quad (5)$$

where, S_{BET} (m^2/g) is the BET surface area of adsorbents, 310.3 is the molecular weight of SDM, N_A is the Avogadro constant, and A_{abs} (g/g) is the amount absorbed at pH 2.0.

The values of A_m obtained from Eq. (5) were 309.7 $Å^2$ (MN-202), 243.4 $Å^2$ (XAD-4), 350.4 $Å^2$ (F-400), 104.5 $Å^2$ (MWCNT without salt), and 55.8 $Å^2$ (MWCNT with $CaCl_2$). This result can be understood from the following two aspects: (1) the availability of surface area on the adsorbents is different. The three porous adsorbents have a much larger BET surface area than MWCNT. However, not all the surfaces of the porous adsorbents were accessible to SDM because SDM molecules are larger than

N_2 molecules, which were used to measure surface area; (2) according to the calculated results and the maximal projection area of the SDM molecule (80.1 Å^2), the SDM molecules adsorbed to the surface of MWCNT are much more close-knit compared with those of other adsorbents (**Fig. 4**).

Moreover, the molecular arrangement changes from being mono-layer to bi-layer at pH 2.0 with the addition of $CaCl_2$, probably because the presence of Ca^{2+} ions affected the adsorption potential of the sulfonamide molecules to the surface of MWCNT by modifying the activity coefficient of sulfonamides. The different effects of ionic strength observed between Na^+ and Ca^{2+} are likely caused by the different abilities of these ions in hydrating, ion pairing, and undertaking complexion in the adsorption process.

2.5 Adsorption isotherms

Adsorption isotherms plotted as adsorbed concentration (q_e, mg/g adsorbent) versus aqueous-phase concentration (C_e, mg/L) at equilibrium are shown in **Fig. 5** (pH = 2.0). All isotherms were nonlinear when the q_e vs. C_e values were plotted on linear coordinates. Therefore, three widely used nonlinear isotherm models, the Freundlich, Langmuir, and Dubinin-Radusckevich models, were employed to fit the experimental data (nonlinear regression) with Origin 7.5 Software (OriginLab Corporation). Only the Langmuir model provided the best fit for all experimental data.

$$q_e = \frac{K_L q_m C_e}{1 + K_L C_e} \tag{6}$$

where, K_L (L/mg) is the adsorption equilibrium constant, which determines the affinity of the adsorbent for the solute and corresponds to the strength of the adsorption; and q_m (mg/g) is the maximum amount of adsorbate per unit weight of the adsorbent to form a complete monolayer on the surface. The Langmuir isotherm equation is derived from simple mass kinetics that assumes the occurrence of chemisorption, which corresponds to the hypothesis of the pseudo second-order model in the dynamic experiment (Subramanyam and Das, 2009). The Langmuir model fits most of the adsorption data very well ($R^2 > 0.99$).

The Langmuir isotherm assumes that the adsorption free energy is independent of both the surface coverage and the formation of a monolayer when the solid surface reaches saturation (Janoš et al., 2003). As calculated above, all the occupied areas per molecule adsorbed on the surface of the adsorbents were greater than their maximal projection area, corresponding to the basic idea behind the Langmuir model on the coverage of the surface by a monomolecular layer. The capacity of the MN-202 (q_m) was found to be the highest of the adsorbents studied. XAD-4 exhibited an adsorption capacity of 217 mg/g, which is clearly higher than that of F-400 (178 mg/g) at pH 2.0. Meanwhile,

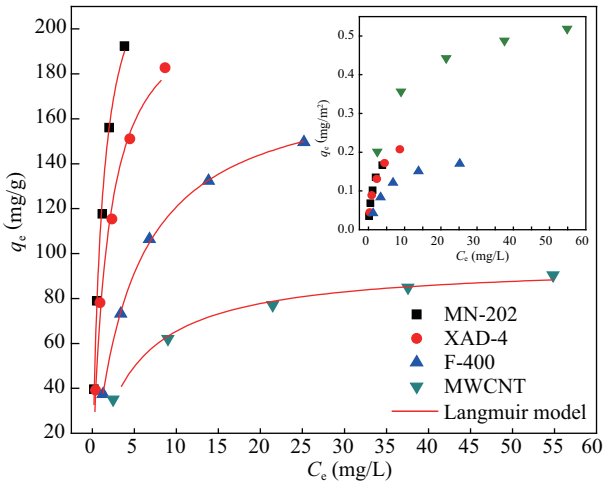

Fig. 5 Adsorption isotherms of SDM by MN-202, XAD-4, F-400 and MWCNT at 303 K and pH 2.0. Inset is adsorption isotherms after surface area normalization.

the capacity of F-400 (q_m) was much greater that that of XAD-4 at pH 8.0. Significant differences were observed among the adsorption isotherms, as q_e was expressed on surface area instead of on mass basis. After the normalization of the surface area (**Fig. 5**, inset), the isotherms of SDM on MWCNT increased at pH 2.0, while that at pH 8.0 was still lower than the others. Therefore, available contact surfaces in the MWCNT were the greatest, able to play a dominant role in the adsorption. MWCNT also provided a cleaner and more cost-effective alternative method by adjusting the aqueous phase pH, and applying weakly acidic conditions in adsorption and basic conditions in desorption (Ji et al., 2009a). Moreover, the selectivity and efficiency of adsorption to MWCNT can be improved by adjusting the pore size distribution and surface area. The current work presents data beneficial in exploring the potential application of engineered adsorbents in associated wastewater treatment.

3 Conclusions

The present work investigated the influence of the main factors potentially controlling antibiotics adsorption to engineered adsorbents: molecule size and partition coefficients K_{ow} and pK_a of adsorbates; specific surface area and pore size of adsorbents; and dynamics and solution chemistry. The results demonstrated that the adsorption of antibiotics to engineered adsorbents is mainly controlled by the specific surface area and pore size of adsorbents along with solution pH values. On a mass basis, the adsorption capacities of MN-202 are higher than those of the other adsorbents due to the hybrid characteristics of the hypercross linked resin, namely, a considerable portion of mesopores and a large quantity of micropores. The results obtained under acidic conditions indicated that MWCNT is more advantageous than the other adsorbents in terms of adsorption capacity as q_e was expressed on surface area

instead of on mass basis. This was due to the ordered, open pore structures of MWCNTs, mesoporous pores, and much more close-knit molecular arrangement on its surface. The present results highlight the importance of considering the surface area and pore structure of engineered adsorbents in predicting the influencing factors in adsorption.

Acknowledgments

We gratefully acknowledge generous support provided by the Key Subject of National Natural Science (No. 50938004), the National Natural Science Foundation of China (No. 51278253), and the Jiangsu Nature Science Fund for Distinguished Scientists (No. BK2010006).

References

Bandosz T J, 2006. Activated Carbon Surfaces in Environmental Remediation Interface Science and Technology, Vol. 7. Elsevier, New York.

Braschi I, Blasioli S, Gigli L, Gessa C E, Alberti A, Martucci A, 2010. Removal of sulfonamide antibiotics from water: Evidence of adsorption into an organophilic zeolite Y by its structural modifications. *Journal of Hazardous Materials*, 178(1-3): 218–225.

Choi K J, Kim S G, Kim S H, 2008. Removal of tetracycline and sulfonamide classes of antibiotic compound by powdered activated carbon. *Environmental Technology*, 29(3): 333–342.

Costa E, Calleja G, Marijuán L, 1988. Comparative adsorption of phenol, *p*-nitrophenol and *p*-hydroxybenzoic acid on activated carbon. *Adsorption Science and Technology*, 5: 213–228.

Domínguez J R, González T, Palo P, Cuerda-Correa E M, 2011. Removal of common pharmaceuticals present in surface waters by Amberlite XAD-7 acrylic-ester-resin: Influence of pH and presence of other drugs. *Desalination*, 269(1-3): 231–238.

Fontecha-Cámara M A, López-Ramón M V, Álvarez-Merino M A, Moreno-Castilla C, 2007. Effect of surface chemistry, solution pH, and ionic strength on the removal of herbicides diuron and amitrole from water by an activated carbon fiber. *Langmuir*, 23(3): 1242–1247.

Gao J A, Pedersen J A, 2005. Adsorption of sulfonamide antimicrobial agents to clay minerals. *Environmental Science and Technology*, 39(24): 9509–9516.

Gao J, Pedersen J A, 2010. Sorption of sulfonamide antimicrobial agents to humic acid-clay complexes. *Journal of Environmental Quality*, 39(1): 228–235.

Janoš P, Buchtová H, Rýznarová M, 2003. Sorption of dyes from aqueous solutions onto fly ash. *Water Research*, 37(20): 4938–4944

Ji L L, Chen W, Bi J, Zheng S R, Xu Z Y, Zhu D Q et al., 2010a. Adsorption of tetracycline on single-walled and multi-walled carbon nanotubes as affected by aqueous solution chemistry. *Environmental Toxicology and Chemistry*, 29(12): 2713–2719.

Ji L L, Chen W, Duan L, Zhu D Q, 2009b. Mechanisms for strong adsorption of tetracycline to carbon nanotubes: A comparative study using activated carbon and graphite as adsorbents. *Environmental Science and Technology*, 43(7): 2322–2327.

Ji L L, Chen W, Zheng S R, Xu Z Y, Zhu D Q, 2009a. Adsorption of sulfonamide antibiotics to multiwalled carbon nanotubes. *Langmuir*, 25(19): 11608–11613.

Ji L L, Liu F L, Xu Z Y, Zheng S R, Zhu D Q, 2010b. Adsorption of pharmaceutical antibiotics on template-synthesized ordered micro-and mesoporous carbons. *Environmental Science and Technology*, 44(8): 3116–22.

Kahle M, Stamm C, 2007a. Sorption of the veterinary antimicrobial sulfathiazole to organic materials of different origin. *Environmental Science and Technology*, 41(1): 132–138.

Kahle M, Stamm C, 2007b. Time and pH-dependent sorption of the veterinary antimicrobial sulfathiazole to clay minerals and ferrihydrite. *Chemosphere*, 68(7): 1224–1231.

Kujawski W, Warszawski A, Ratajczak W, Porebski T, Capała W, Ostrowska I, 2004. Removal of phenol from wastewater by different separation techniques. *Desalination*, 163(1-3): 287–296.

Kurwadkar S T, Adams C D, Meyer M T, Kolpin D W, 2007. Effects of sorbate speciation on sorption of selected sulfonamides in three loamy soils. *Journal of Agricultural and Food Chemistry*, 55(4): 1370–1376.

Oleszczuk P, Pan B, Xing B S, 2009. Adsorption and desorption of oxytetracycline and carbamazepine by multiwalled carbon nanotubes. *Environmental Science and Technology*, 43(24): 9167–9173.

Rabie U M, Abou-Ei-Wafa M H, Mohamed R A, 2007. Interaction of 2-aminopyrimidine with σ- and π-acceptors involving chemical reactions via initial charge transfer complexation. *Journal of Molecular Structure*, 871(1-3): 6–13.

Richter M K, Sander M, Krauss M, Christl I, Dahinden M G, Schneider M K et al., 2009. Cation binding of antimicrobial sulfathiazole to leonardite humic acid. *Environmental Science and Technology*, 43(17): 6632–6638.

Sanders S M, Srivastava P, Feng Y, Dane J H, Basile J, Barnett M O, 2008. Sorption of the veterinary antimicrobials sulfadimethoxine and ormetoprim in soil. *Journal of Environment Quality*, 37(4): 1510–1518.

Schwarzenbach R P, Gschwend P M, Imboden D M, 1993. Environmental Organic Chemistry. John Wiley & Sons, New York. 681.

Subramanyam B, Das A, 2009. Linearized and non-linearized isotherm models comparative study on adsorption of aqueous phenol solution in soil. *International Journal of Environment Science and Technology*, 6(4): 633–640.

Sukul P, Lamshöt M, Zühlke S, Spiteller M, 2008. Sorption and desorption of sulfadiazine in soil and soil-manure systems. *Chemosphere*, 73(8): 1344–1350.

Ternes T A, Joss A, Siegrist H, 2004. Scrutinizing pharmaceuticals and personal care products in wastewater treatment. *Environmental Science and Technology*, 38(20): 392A–399A.

Thiele-Bruhn S, Seibicke T, Schulten H R, Leinweber P, 2004. Sorption of sulfonamide pharmaceutical antibiotics on whole soils and particle-size fractions. *Journal of Environmental Quality*, 33(4): 1331–1342.

Tolls J, 2001. Sorption of veterinary pharmaceuticals in soils:

a review. *Environmental Science and Technology*, 35(17): 3397–3406.

Valderrama C, Barios J I, Farran A, Cortina J L, 2011. Evaluation of phenol/aniline (single and binary) removal from aqueous solutions onto hyper-cross-linked polymeric resin (Macronet MN200) and granular activated carbon in fixed-bed column. *Water, Air, and Soil Pollution*, 215(1-4): 285–297.

Vinu A, Hossain K Z, Kumar G S, Ariga K, 2006. Adsorption of l-histidine over mesoporous carbon molecular sieves. *Carbon*, 44(3): 530-536.

Wibowo N, Setyadhi L, Wibowo D, Setiawan J, Ismadji S, 2007. Adsorption of benzene and toluene from aqueous solutions onto activated carbon and its acid and heat treated forms: Influence of surface chemistry on adsorption. *Journal of Hazardous Materials*, 146(1-2): 237–242.

Yang K, Wu W B, Jing Q F, Jiang W, Xing B S, 2010. Competitive adsorption of naphthalene with 2,4-dichlorophenol and 4-chloroaniline on multiwalled carbon nanotubes. *Environmental Science and Technology*, 44(8): 3021–3027.

Yang K, Xing B S, 2010. Adsorption of organic compounds by carbon nanomaterials in aqueous phase: polanyi theory and its application. *Chemical Reviews*, 110(10): 5989–6008.

Yang W B, Li A M, Fu C, Fan J, Zhang Q X, 2007. Adsorption mechanism of aromatic sulfonates onto resins with different matrices. *Industrial and Engineering Chemistry Research*, 46(21): 6971–6977.

Zhang D, Pan B, Zhang H, Ning P, Xing B S, 2010. Contribution of different sulfamethoxazole species to their overall adsorption on functionalized carbon nanotubes. *Environmental Science and Technology*, 44(10): 3806–3811.

Zhou J L, 2006. Sorption and remobilization behavior of 4-*tert*-octylphenol in aquatic systems. *Environmental Science and Technology*, 40(7): 2225–2234.

JOURNAL OF ENVIRONMENTAL SCIENCES

环境科学学报(英文版)

(http://www.jesc.ac.cn)

Aims and scope

Journal of Environmental Sciences is an international academic journal supervised by Research Center for Eco-Environmental Sciences, Chinese Academy of Sciences. The journal publishes original, peer-reviewed innovative research and valuable findings in environmental sciences. The types of articles published are research article, critical review, rapid communications, and special issues.

The scope of the journal embraces the treatment processes for natural groundwater, municipal, agricultural and industrial water and wastewaters; physical and chemical methods for limitation of pollutants emission into the atmospheric environment; chemical and biological and phytoremediation of contaminated soil; fate and transport of pollutants in environments; toxicological effects of terrorist chemical release on the natural environment and human health; development of environmental catalysts and materials.

For subscription to electronic edition

Elsevier is responsible for subscription of the journal. Please subscribe to the journal via http://www.elsevier.com/locate/jes.

For subscription to print edition

China: Please contact the customer service, Science Press, 16 Donghuangchenggen North Street, Beijing 100717, China. Tel: +86-10-64017032; E-mail: journal@mail.sciencep.com, or the local post office throughout China (domestic postcode: 2-580).

Outside China: Please order the journal from the Elsevier Customer Service Department at the Regional Sales Office nearest you.

Submission declaration

Submission of an article implies that the work described has not been published previously (except in the form of an abstract or as part of a published lecture or academic thesis), that it is not under consideration for publication elsewhere. The submission should be approved by all authors and tacitly or explicitly by the responsible authorities where the work was carried out. If the manuscript accepted, it will not be published elsewhere in the same form, in English or in any other language, including electronically without the written consent of the copyright-holder.

Submission declaration

Submission of the work described has not been published previously (except in the form of an abstract or as part of a published lecture or academic thesis), that it is not under consideration for publication elsewhere. The publication should be approved by all authors and tacitly or explicitly by the responsible authorities where the work was carried out. If the manuscript accepted, it will not be published elsewhere in the same form, in English or in any other language, including electronically without the written consent of the copyright-holder.

Editorial

Authors should submit manuscript online at http://www.jesc.ac.cn. In case of queries, please contact editorial office, Tel: +86-10-62920553, E-mail: jesc@263.net, jesc@rcees.ac.cn. Instruction to authors is available at http://www.jesc.ac.cn.

Journal of Environmental Sciences (Established in 1989)

Vol. 25 No. 7 2013

Supervised by	Chinese Academy of Sciences	**Published by**	Science Press, Beijing, China
Sponsored by	Research Center for Eco-Environmental		Elsevier Limited, The Netherlands
	Sciences, Chinese Academy of Sciences	**Distributed by**	
Edited by	Editorial Office of Journal of	Domestic	Science Press, 16 Donghuangchenggen
	Environmental Sciences		North Street, Beijing 100717, China
	P. O. Box 2871, Beijing 100085, China		Local Post Offices through China
	Tel: 86-10-62920553; http://www.jesc.ac.cn	Foreign	Elsevier Limited
	E-mail: jesc@263.net, jesc@rcees.ac.cn		http://www.elsevier.com/locate/jes
Editor-in-chief	Hongxiao Tang	**Printed by**	Beijing Beilin Printing House, 100083, China

CN 11-2629/X **Domestic postcode: 2-580** **Domestic price per issue RMB ¥ 110.00**

ISSN 1001-0742